

Modified SPIHT algorithm for wavelet packet image coding

Nikola Sprljan^{a,*}, Sonja Grgic^b, Mislav Grgic^b

^a*Multimedia and Vision Lab, Department of Electronic Engineering, Queen Mary, University of London, London E1 4NS, UK*

^b*Faculty of Electrical Engineering and Computing, University of Zagreb, Unska 3/XII, HR-10000 Zagreb, Croatia*

Available online 10 August 2005

Abstract

This paper introduces a new implementation of wavelet packet decomposition which is combined with SPIHT (Set Partitioning in Hierarchical Trees) compression scheme. We provide the analysis of the problems arising from the application of zerotree quantisation based algorithms (such as SPIHT) to wavelet packet transform coefficients. We established the generalized parent–child relationships for wavelet packets, providing complete tree structures for SPIHT. The proposed algorithm can be used for both wavelet dyadic and Wavelet Packet decomposition (WP-SPIHT). An extensive evaluation of the algorithm was performed and it has been shown that WP-SPIHT significantly outperforms base-line SPIHT coder for texture images. For these images the suboptimal WP cost-function enables good enough energy compaction that is efficiently exploited by the WP-SPIHT.

© 2005 Elsevier Ltd. All rights reserved.

1. Introduction

Discrete Wavelet Transform (DWT) provides a multiresolution image representation and has become one of the most important tools in image analysis and coding over the last two decades. Image compression algorithms based on DWT [1–8] provide high coding efficiency for natural (smooth) images. As dyadic DWT does not adapt to the various space-frequency properties of images, the energy compaction it achieves is generally not optimal. However, the performance can be improved by selecting the transform basis adaptively to the image. Wavelet Packets (WP) represent a generalization of wavelet decomposition scheme. WP image decomposition adaptively selects a transform basis that will be best suited to the particular image. To achieve that, the criterion for best basis selection is needed.

Coifman and Wickerhauser proposed entropy based algorithm for best basis selection [9]. In their work, the best basis is a basis that describes the particular image with the smallest number of basis functions. It is a one-

sided metric, which is therefore not optimal in a joint rate-distortion sense. A more practical metric considers the number of bits (rate) needed to approximate an image with a given error (distortion) [10] but this approach and its variation presented in [11] can be computationally too intensive. In [12] a fast numerical implementation of the best wavelet packet algorithm is provided. Coding results show that fast wavelet packet coder can significantly outperform a sophisticated wavelet coder constrained to using only a dyadic decomposition, with a negligible increase in computational load.

The goal of this paper is to demonstrate advantages and disadvantages of using WP decomposition in SPIHT-based codec. SPIHT algorithm was introduced by Said and Pearlman [13], and is improved and extended version of Embedded Zerotree Wavelet (EZW) coding algorithm introduced by Shapiro [14]. Both algorithms work with tree structure, called Spatial Orientation Tree (SOT), that defines the spatial relationships among wavelet coefficients in different decomposition subbands. In this way, an efficient prediction of significance of coefficients based on significance of their “parent” coefficients is enabled. The main contribution of Shapiro’s work is zerotree quantization of wavelet

*Corresponding author.

E-mail address: nikola@sprljan.com (N. Sprljan).

URL: <http://www.sprljan.com/nikola>.

coefficients and introduction of special zerotree symbol indicating that all coefficients in a SOT are found to be insignificant with respect to a particular quantization threshold. An embedded zerotree quantizer refines each input coefficient sequentially using a bitplane coding scheme, and it stops when the size of the encoded bitstream reaches the target bit-rate. SPIHT coder provides gain in PSNR over EZW due to introduction of a special symbol that indicates significance of child nodes of a significant parent and separation of child nodes (direct descendants) from second-generation descendants. To date, there have been numerous variants and extensions to SPIHT algorithm, for example: 3-D SPIHT for video coding [15–19], SPIHT for color image coding [20,21], and scalable SPIHT for network applications [22–25].

Since the SPIHT algorithm relies on Spatial Orientation Trees (SOT) defined on dyadic subband structure, there are a few problems that arise from their adaptation to WP decomposition. First is the so-called *parental conflict* [26], that happens when in the wavelet packet tree one or more of the child nodes are at the coarser scale than the parent node. It must be resolved in order that SOT structure with well-defined parent–child relationships for an arbitrary wavelet decomposition can be created. Xiong et al. [11] avoided the parental conflict by restricting the choice of the basis. In their work the Space-Frequency Quantization (SFQ) algorithm is used. SFQ algorithm employs a rate-distortion (R-D) optimization framework for selecting the best basis and to assign an optimal quantiser to each of the wavelet packet subbands. Rajpoot et al. [26] defined a set of rules to construct the zerotree structure for a given wavelet packet geometry and offered a general structure for an arbitrary WP decomposition. In their work a Compatible Zerotree Quantisation (CZQ) is utilized, and it does not impose restriction on the selection of WP basis. A comparison of PSNR obtained with CZQ-WP and SPIHT shows that SPIHT provides gain in PSNR over CZQ-WP for the standard test images, while CZQ-WP offers better visual quality than SPIHT [26]. This observation motivated us to use SPIHT with WP in order to exploit strengths of both methods. This extension of SPIHT we call Wavelet Packet SPIHT (WP-SPIHT).

This paper is organized as follows: In Section 2 wavelet analysis in the context of WP-SPIHT is described. In Section 3 we explain WP-SPIHT algorithm. Coding results are presented in Section 4, followed by conclusion in Section 5.

2. Wavelet analysis

Wavelet analysis of an image can be viewed in the frequency domain as partitioning into a set of subbands,

where each partitioning step is obtained by applying the 2D wavelet transform. One level of 2D wavelet transform results in four sets of data (wavelet coefficients), that correspond to four 2D frequency subbands. For these four subbands, if the original image data is on the zero decomposition level (scale), we use the following notation on k th decomposition level: HH_k (high–high or diagonal details), HL_k (high–low or horizontal details), LH_k (low–high or vertical details), LL_k (low–low or approximation). LL_k subband is also called image approximation as it represents image on a lower scale, while to other subbands we refer as to image details. Wavelet decomposition is dyadic in a case when only the LL_k subband is further transformed. It results in a new set of subbands: HH_{k+1} , HL_{k+1} , LH_{k+1} , LL_{k+1} . Dyadic decomposition used in image compression will thus generate hierarchical pyramidal structure, as shown in Fig. 1. If the dyadic decomposition of N levels is performed (N times transforming the low–low subband) the result will be $3N + 1$ subbands. The WP decomposition is a generalization of wavelet dyadic decomposition, where further wavelet transform on detail subbands is possible, potentially producing up to 4^N final subbands. A single wavelet packet decomposition thus provides a multitude of choices from which the best representation with respect to a design objective (e.g. compression efficiency) can be found.

In order to achieve compression gain while keeping the computational load reasonably low, two entities are needed: a criterion (cost function) for basis comparison and a fast search algorithm, which finds the best basis from the set of all possible bases. The best basis can be selected using either entropy based cost, as proposed in

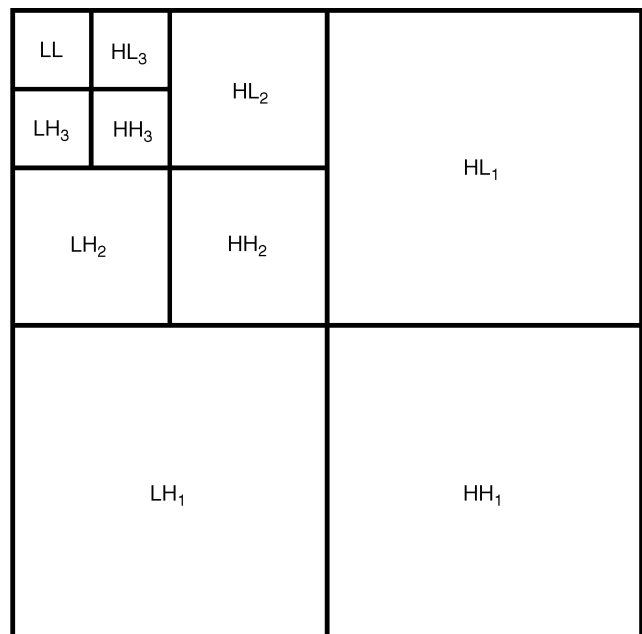


Fig. 1. Pyramidal structure of 3-level wavelet decomposition.

[9], or by jointly estimating the rate-distortion function, as in [10], but whichever method is selected it does not explicitly define the parent–child relationships in produced wavelet subbands. The overall complexity of the approach in [10] is extremely high, because the selection of best basis involves three embedded nonlinear optimization problems. In [9] several cost functions based on entropy criterion were defined (Shannon, Logarithm of Energy, l -Norm and Threshold), but Shannon entropy was found as most attractive. Therefore, in this work we use Shannon entropy of wavelet coefficients as cost function for WP bases comparison. The cost is expressed in terms of bits and it provides fast and fairly accurate estimation of the actual output bits that will be spent in coding of the coefficients. In order to find the best basis we apply adaptive search using single spatial tree algorithm, [10,27]. There are two possible approaches for finding the best tree [27]: fully grown tree and “greedy” grown tree. To compare complexity of each one the following notation is introduced here: $L \times L$ is the size of a square image, N is the maximum allowed depth of the decomposition, α_0 is the constant specifying per-pixel complexity of DWT for a wavelet filter of a specific length, and α_1 is the constant specifying per-pixel complexity of the computation of the specific cost measure. With this notation the complexity of the dyadic wavelet transform f_D is

$$f_D = \sum_{k=0}^{N-1} \alpha_0 (2^{-k}L)^2 = \alpha_0 \frac{4^{N-1} - 1}{3 \times 4^{N-2}} L^2 \leq \alpha_0 \frac{4}{3} L^2. \quad (1)$$

Since the decomposition is fixed, no computation of cost measure is necessary and the complexity is dependent only on α_0 . In a case where the full growth is employed, the best basis is searched over all possible bases. With respect to the given cost measure, the optimal basis can always be found. If all the intermediate subbands are preserved, i.e. the implementation is not in place, it can be shown that the complexity of a full growth f_F is

$$f_F = (\alpha_0 N + \alpha_1 (N + 1)) L^2. \quad (2)$$

In this case the complexity is independent of the finally selected tree. The complexity of the greedy approach f_G is

$$f_G = (\alpha_0 (1 + r_t) + \alpha_1 (2 + r_t)) L^2, \quad (3)$$

where $0 \leq r_t \leq N - 1$ is the factor that depends on the finally selected tree. When the greedy search happens to grow the decomposition tree up to the fully grown tree, then $r_t = N - 1$ and $f_G = f_F$. Depending on the source image, the complexity generally falls between the two specified extremes. Thus, greedy approach is in general computationally less complex on the expense of potentially suboptimal performance.

In the proposed implementation, each of the N steps of the dyadic wavelet decomposition is followed by the

greedy growing tree algorithm on the obtained high-pass subbands. The growth of the tree is controlled with parameter $d \leq N$, that defines the coarsest scale of the subband that can be produced by the greedy growth. Each subband that is on the scale finer than d is decomposed depending on the decision given by the cost function. The complexity for this type of decomposition is upper bounded with

$$\begin{aligned} f_{G'_u} &= f_D + 3 \left(\alpha_0 \sum_{k=1}^{d-1} 2^{-2k} (d - k) \right. \\ &\quad \left. + \alpha_1 \sum_{k=1}^{d-1} 2^{-2k} (d - k + 1) \right) L^2 \\ &= f_D + \frac{1}{3} \left(\alpha_0 \left(\frac{1}{4^{d-1}} + 3d - 4 \right) \right. \\ &\quad \left. + \alpha_1 \left(\frac{-2}{4^{d-1}} + 3d - 1 \right) \right) L^2 \\ &\leq \left(\alpha_0 \left(d + \frac{4}{3} \right) + \alpha_1 d \right) L^2. \end{aligned} \quad (4)$$

It can be seen that the complexity increases linearly with d . The lower bound of the complexity, for the case when only the immediately lower level of the dyadic decomposition tree is grown, is given by

$$\begin{aligned} f_{G'_l} &= f_D + 3(\alpha_0 + 2\alpha_1) \sum_{k=1}^{d-1} 2^{-2k} L^2 \\ &= f_D + \frac{4^{d-1} - 1}{4^{d-1}} (\alpha_0 + 2\alpha_1) L^2 \approx 2f_D. \end{aligned} \quad (5)$$

Since the algorithm execution time largely depends on the wavelet transform, this determines the overall WP-SPIHT execution time to be at least two times longer than for the baseline SPIHT.

Pseudocodes for WP decomposition/reconstruction and greedy tree growth algorithm are given in Tables 1–3. Dyadic wavelet decomposition interleaved with greedy growth decomposition of the high-pass subbands is defined by function “Decompose” (Table 1), where the greedy growth itself is performed with the function “WPanalysis” (Table 2). The “treeinfo” vector contains a description of the chosen basis and is necessary at the decoder for proper reconstruction. This information represents a bit-stream overhead, but its influence on compression results is negligible. Note that when $d = 0$ this is equivalent to performing only dyadic decomposition and in this case the WP-SPIHT coder produces results identical to the baseline SPIHT coder. SOTs are dynamically built during the decomposition. This is in the pseudocodes represented by the operations “define parent–children relations” and “resolve parental conflicts”, which are explained in Section 3. The image is reconstructed as shown in Table 3, using function “Reconstruct” for dyadic reconstruction, and, as

Table 1
Pseudocode for wavelet packets decomposition

```

function Decompose(image, N, d) → {S, costimage, treeinf}
image → LL0
0 → costimage
[] → treeinf
for k = 1 to N
  DWT(LLk-1) → [[LLk HLk]T[LHk HHk]T] → LLk-1
  if k < d
    WPanalysis(HLk, d - k, treeinf) → {HLk, costHL, treeinf}
    WPanalysis(LHk, d - k, treeinf) → {LHk, costLH, treeinf}
    WPanalysis(HHk, d - k, treeinf) → {HHk, costHH, treeinf}
  else
    cost(HLk) → costHLk
    cost(LHk) → costLHk
    cost(HHk) → costHHk
    costimage + costHLk + costLHk + costHHk → costimage
  define parent–children relations
  resolve parental conflicts
costimage + cost(LLN) → costimage
LL0 → S ≡ ⋃k=1N (HLk, LHk, HHk), LLN
    
```

Table 2
Pseudocode for greedy tree growth algorithm

```

function WPanalysis(S, depth, treeinf) → {S, costS, treeinf}
DWT(S) → [[LL HL]T[LH HH]T] → S
cost(S) → costS
cost(LL) → costLL
cost(HL) → costHL
cost(LH) → costLH
cost(HH) → costHH
if costLL + costHL + costLH + costHH < costS
  if depth > 1
    WPanalysis(LL, depth - 1, treeinf) → {LL, costLL, treeinf}
    WPanalysis(HL, depth - 1, treeinf) → {HL, costHL, treeinf}
    WPanalysis(LH, depth - 1, treeinf) → {LH, costLH, treeinf}
    WPanalysis(HH, depth - 1, treeinf) → {HH, costHH, treeinf}
  [1 treeinf] → treeinf
  costLL + costHL + costLH + costHH → costS
  [[LL HL]T[LH HH]T] → S
else [0 treeinf] → treeinf
    
```

specified by the “treeinfo” parameter, the function “WPsynthesis” performs WP reconstruction.

3. Definition of SOTs in WP-SPIHT

SPIHT algorithm exploits the statistical properties of pyramid wavelet transformed image, which are energy compaction, cross-subband similarity and decaying of coefficient magnitudes across subbands. Fig. 2 indicates the SOTs and corresponding parent–children relationships across the subbands in the case of the dyadic

Table 3
Pseudocode for wavelet packets reconstruction

```

function Reconstruct(S, N, d, treeinf) → image
for k = N to 1
  if k < d
    WPsynthesis(HHk, d - k, treeinf) → HHk
    WPsynthesis(LHk, d - k, treeinf) → LHk
    WPsynthesis(HLk, d - k, treeinf) → HLk
  IDWT(LLk, HLk, LHk, HHk) → LLk+1
LL0 → image

function WPsynthesis(S, depth, treeinf) → S
if treeinf1 == 1
  remove treeinf1 from treeinf
  S → [[LL HL]T[LH HH]T]
  if depth > 1
    WPsynthesis(HH, depth - 1, treeinf) → {HH, treeinf}
    WPsynthesis(LH, depth - 1, treeinf) → {LH, treeinf}
    WPsynthesis(HL, depth - 1, treeinf) → {HL, treeinf}
    WPsynthesis(LL, depth - 1, treeinf) → {LL, treeinf}
  IDWT(LL, HL, LH, HH) → S
else remove treeinf1 from treeinf
    
```

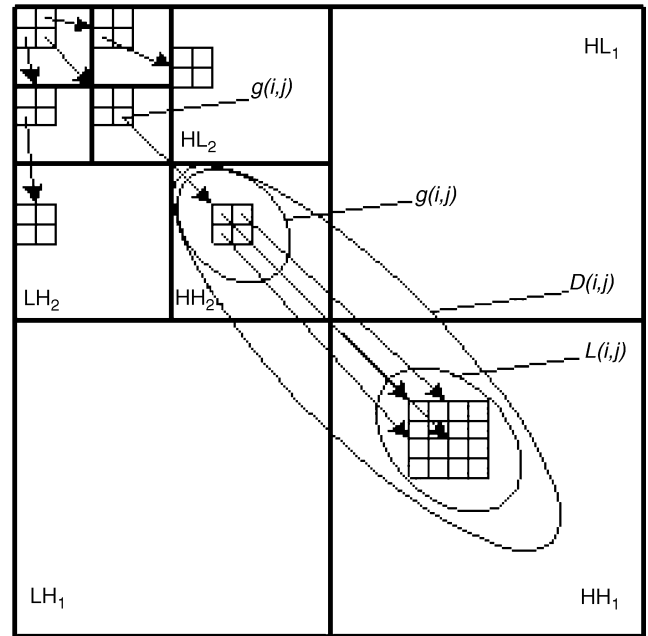


Fig. 2. Parent–children relations across subbands.

decomposition. In the text that follows, a wavelet transform coefficient is also referred to as a “pixel”. Let $c(i, j)$ denote the wavelet transform coefficient (pixel) at (row, column) position in the transformed image. The set of immediate descendants (children) of a coefficient is denoted by $O(i, j)$, the set of all descendants $D(i, j)$, and the set of all descendants, but excluding immediate children is $L(i, j) = D(i, j) \setminus O(i, j)$, Fig. 2. If $c(1, 1)$ is pixel

in the upper left corner of the image, for the dyadic decomposition the set O is defined as $O(i, j) = \{(2i - 1, 2j - 1), (2i - 1, 2j), (2i, 2j - 1), (2i, 2j)\}$ (for LH_n, HL_n and HH_n subbands, $n = 2 \dots N$). For LL_N the set O can be defined in several ways with negligible variations in compression performance. Here the definition as in EZW is selected, where $O(i, j) = \{(i, 2j - 1), (2i - 1, j), (2i - 1, 2j - 1)\}$. For the case of the WP decomposition, the parent–child relations have to be adapted in a way that the property of cross-level similarities is preserved. *Dyadic decomposition level* of a certain subband is defined, and its value is the same as of the initial dyadic subband from which it has been obtained by further decomposition, e.g. all subbands obtained from decomposing LH_1 are at the same dyadic decomposition level. Therefore, the same dyadic decomposition level does not implicate the same scale—just the same position on a dyadic wavelet tree.

The examples of parent–child assignments are shown in Fig. 3, where each subband is marked with a dot whose radius is inversely proportional to its scale. If the whole subband is treated as node in a SOT, Natural Parent (NP) can be defined as an SOT node whose child is on the immediately finer scale. A child of an NP must have the same relative position as NP, if a relative position of subband is defined in regard to initial dyadic subband from which it is obtained by further decomposition. With regular SOTs, as in SPIHT, each parent coefficient has four of its children on the same spatial location and immediately on next lower level of wavelet decomposition tree. Therefore all parents in dyadic wavelet decompositions are natural, Fig. 3(a). With WP

decomposition the parent–child assignments are more complex since that there can be various scale differences between subbands on adjacent dyadic decomposition levels. In contrast to dyadic decomposition, in the wavelet packet tree one or more of the child nodes can be at the coarser scale than the parent node. Two types of parental conflict can arise:

- (1) Type 1—When a coefficient in a child node can be associated to multiple parent coefficients in the parent node.
- (2) Type 2—When more than four coefficients in a child node can be children coefficients to a coefficient in the parent node.

Let R denote the node representing the lowest frequency subband (LL_N) in the top-left corner of a dyadic decomposed image, Fig. 3(b). It has three children represented with nodes T_1, T_2 and T_3 , which correspond to the coarsest scale high-frequency subbands HL_N, LH_N and HH_N . These are the root nodes of three compatible SOTs with different orientations—horizontal, vertical and diagonal, respectively. All subbands on next lower level are here called child subbands, although when parental conflicts are resolved, a real parent can be found in some upper level. Four different cases of inter-level dependencies can be recognized:

- (1) A subband has within the same relative position child subbands which are on a coarser scale (parental conflict, type 1); example is the subtree of T_2 and child subbands C_1, C_2, C_3, C_4 , Fig. 3(b).
- (2) A subband has within the same relative position child subband that is on the same scale; example is the subtree of T_2 , Fig. 3(b).
- (3) A subband has within the same relative position child subband that is on a immediately finer scale; example is the subtree of T_3 (NP-natural parent–child relation), Fig. 3(b).
- (4) Relative position of subband overlaps with the relative position of a child subband that is on a scale more than one level finer (parental conflict, type 2); example is the subtree of T_1 , Fig. 3(b).

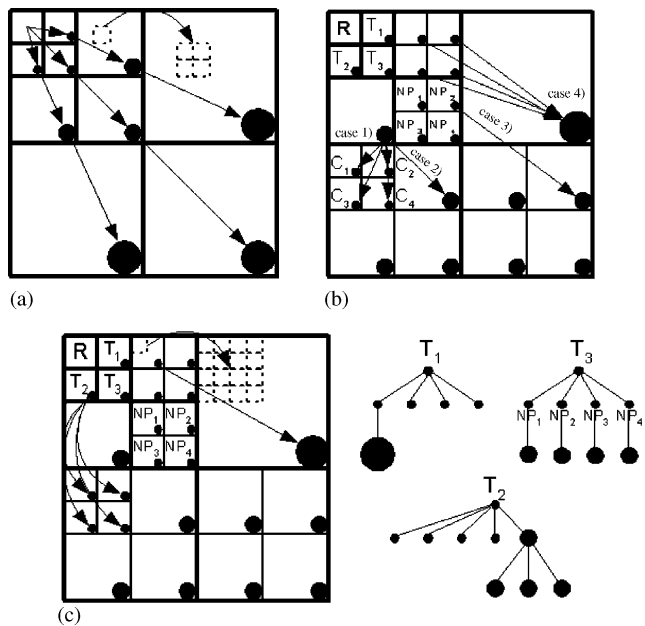


Fig. 3. Examples of parent–child assignments: (a) wavelet decomposition tree, (b) wavelet packet trees and inter-level dependencies, (c) parent–child assignments after resolving the parental conflicts.

In [11] only wavelet trees with cases (2) and (3) were considered. In [26] case (1) is resolved by moving up in the tree all subbands on a lower level that caused the parental conflict, until the conflict is resolved, i.e. until case (1) turns to (2) or (3). In case (2) there is only one child per parent, as the involved subbands are on the same scale. We adopted the same approach for these two cases, but we also consider case (4) which we resolved by assigning the child subband to the first subband on higher level that is found within same relative position, using some predefined scanning order. In that case one node can have more than four children,

specifically, the number of children becomes 4^n , n being the difference in scales between parent and child node. The required modification of SPIHT is introduced that enables support for parents having any number of children, thus covering cases (2) and (4). Fig. 3(c) shows examples of parent–child assignments after resolving the parental conflicts. The conflicts arisen after one step of dyadic decomposition and subsequent greedy growth of the high-pass subbands, are resolved before performing next level of the dyadic decomposition, as shown in Table 1.

4. Experimental results

WP-SPIHT algorithm has been tested on eight 512×512 images: “Goldhill”, “Lena”, “Barbara”, “Fingerprints”, “Zone” and three textures from the “Brodatz” album [28]—“D49”, “D76” and “D106”. Biorthogonal 9/7 transform is used for wavelet packets decomposition. Fig. 4 shows examples of best basis geometry from the experiments. The software used in experiments is available at [29].

We present WP-SPIHT and SPIHT coding results both visually and in the terms of PSNR. For natural images “Lena”, “Goldhill” and “Barbara” PSNR results for SPIHT are better than for WP-SPIHT, Figs. 5–7, while WP-SPIHT provides better visual quality for textured parts of these images. We use the term ‘texture’ to describe region of the image composed of repetitive and approximately periodic patterns which are small in comparison to region’s size. To demonstrate the performance, Figs. 8–11 compare visual quality of SPIHT and WP-SPIHT decoded images “Barbara” and “Goldhill”.

Representation of finely textured regions is noticeably better for WP-SPIHT algorithm, Fig. 9. In Fig. 11(b) it can be seen that texture of the roof has been erased by

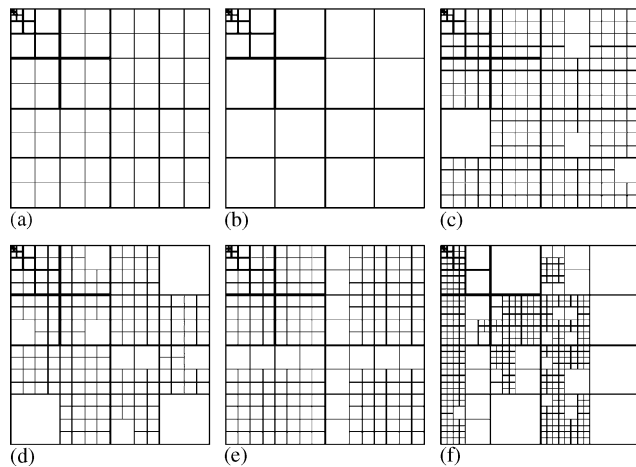


Fig. 4. Best basis geometry: (a) Goldhill, (b) Lena, (c) Barbara, (d) Fingerprints, (e) Zone, (f) D49.

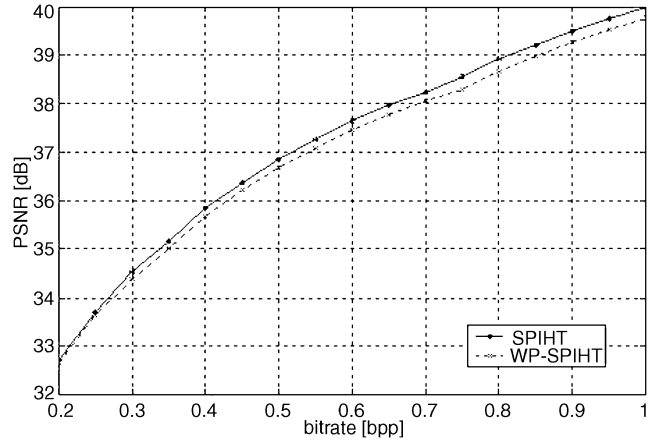


Fig. 5. Lena: comparison of PSNR values for SPIHT and WP-SPIHT.

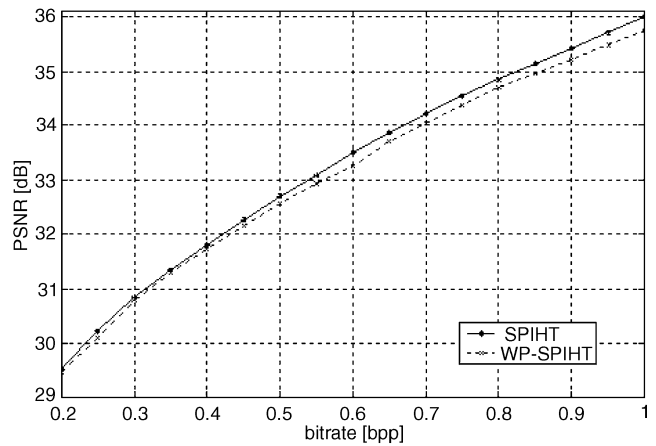


Fig. 6. Goldhill: comparison of PSNR values for SPIHT and WP-SPIHT.

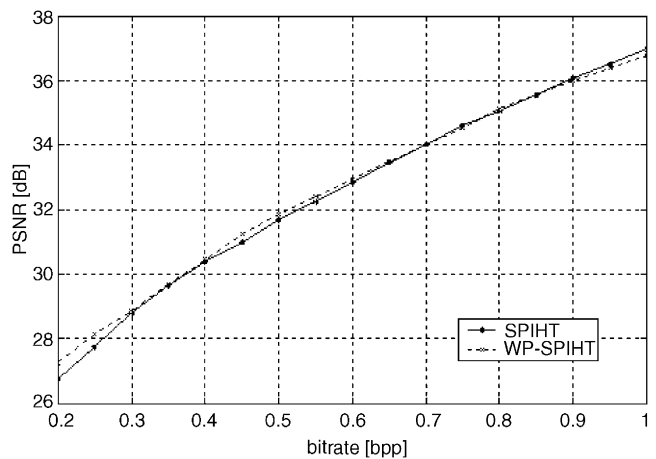


Fig. 7. Barbara: comparison of PSNR values for SPIHT and WP-SPIHT.



Fig. 8. (a) Original image Barbara, (b) SPIHT decoded, 0.25 bpp, (c) WP-SPIHT decoded, 0.25 bpp.

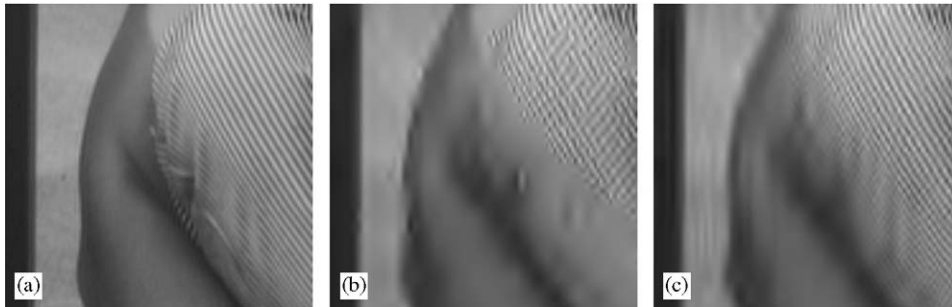


Fig. 9. Magnified detail from image Barbara: (a) original, (b) SPIHT decoded, 0.25 bpp, (c) WP-SPIHT decoded, 0.25 bpp.



Fig. 10. (a) Original Goldhill, (b) SPIHT decoded, 0.25 bpp, (c) WP-SPIHT decoded, 0.25 bpp.



Fig. 11. Magnified detail from image Goldhill: (a) original, (b) SPIHT decoded, 0.25 bpp, (c) WP-SPIHT decoded, 0.25 bpp.

SPIHT, while WP-SPIHT has preserved it, Fig. 11(c). Wavelet packet basis can represent waveforms that are very well localized in frequency and therefore can be

very well fitted for a particular image since it can match oscillatory patterns of image textures. For images that contain a mixture of smooth and textured features

WP-SPIHT yields lower PSNR than SPIHT, but textured parts of these images have better visual quality for WP-SPIHT than for SPIHT. Ringing artefacts are visible for both SPIHT and WP-SPIHT at sharp edges where the intensity abruptly changes. Wavelet coefficients of a large magnitude in the high-pass subbands can be observed on locations corresponding to the edges in the image. The error caused by quantization of these coefficients will cause phenomenon of ringing artefacts that are localized around the affected edges. In the WP case, quantization of these coefficients can affect large regions around edges since the support of wavelet filters operating on high-pass wavelet coefficients is increased.

WP-SPIHT algorithm outperforms SPIHT in terms of PSNR for “Fingerprints”, synthetic image “Zone” and images of textures, Figs. 12–16. Compression results for synthetic image “Zone” with oscillatory pattern and three textures from the “Brodatz” album demonstrate the property of WP-SPIHT algorithm of reproducing oscillatory patterns and textures. The basis selected by the algorithm is usually well adapted to the target image,

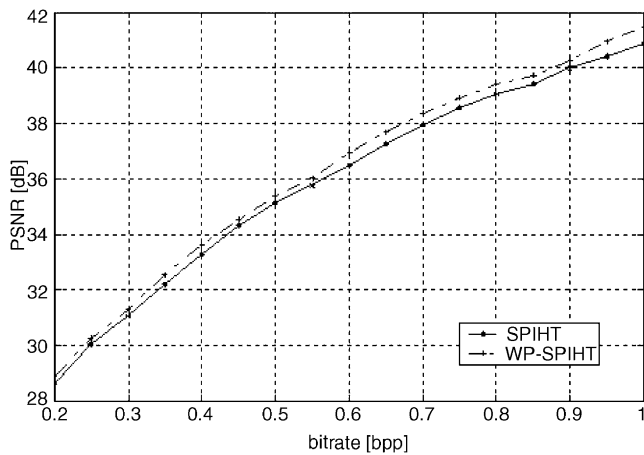


Fig. 12. Fingerprints: comparison of PSNR values for SPIHT and WP-SPIHT.

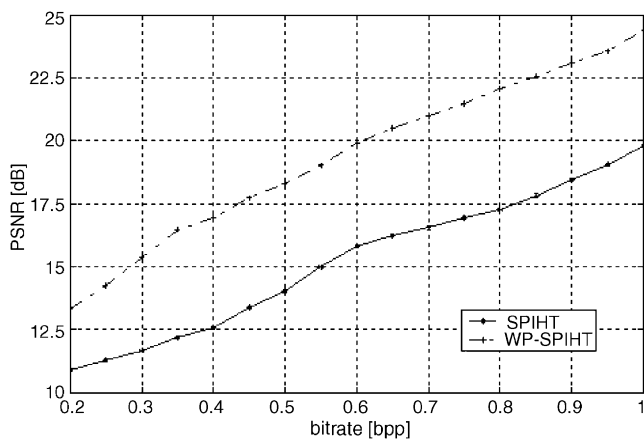


Fig. 13. Zone: comparison of PSNR values for SPIHT and WP-SPIHT.

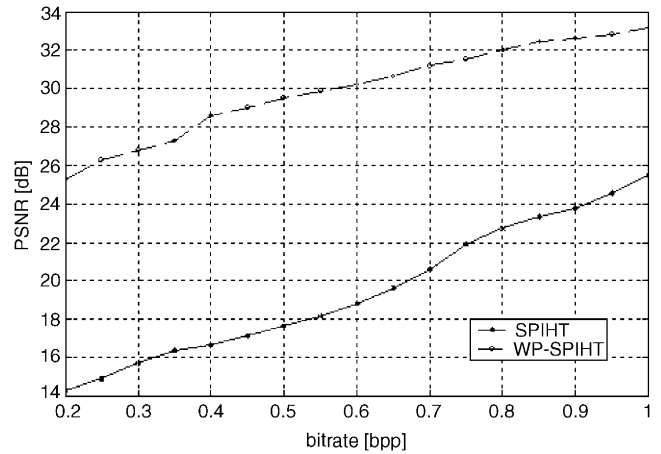


Fig. 14. Texture D49: comparison of PSNR values for SPIHT and WP-SPIHT.

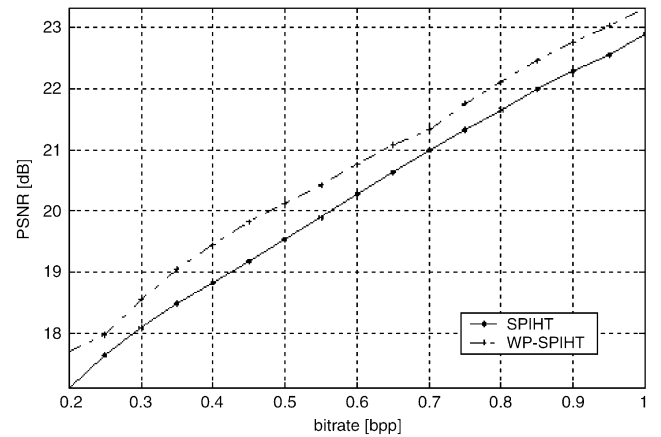


Fig. 15. Texture D76: comparison of PSNR values for SPIHT and WP-SPIHT.

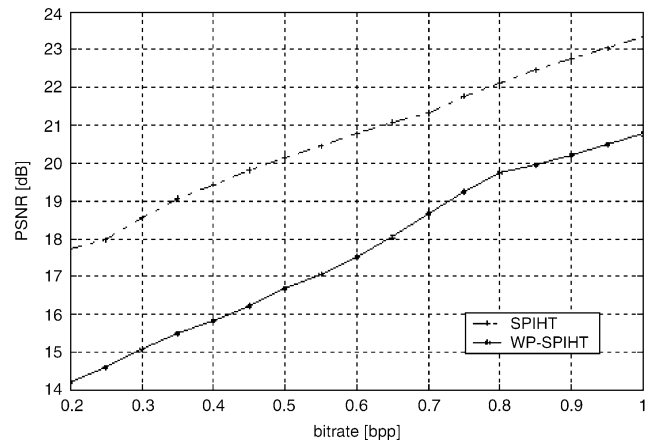


Fig. 16. Texture D106: comparison of PSNR values for SPIHT and WP-SPIHT.

and with the WP-SPIHT coder it is possible to obtain much crisper reconstructed image than with the SPIHT coder.

Images “Fingerprints” and “Zone” contain oscillatory patterns in the vertical, horizontal and diagonal directions. Zone contains concentric circular pattern with monotonic increase in frequency towards borders of the image. Improvement of WP-SPIHT algorithm is less significant for “Fingerprints” (0.1–0.3 dB) than for “Zone” (2.5–4 dB), Figs. 12 and 13. WP-SPIHT coder persistently outperforms SPIHT for compressing textures, Figs. 14–16. Figs. 17–19 show the result of a compression using SPIHT and WP-SPIHT at the same compression rate (0.25 bpp) for images “Fingerprints”, “Zone” and texture “D49”, respectively. We notice in

Fig. 18 that WP-SPIHT image has much better visual quality than SPIHT image in the corners of image Zone that contain high frequency alternations of black and white lines, but in the center of this image (low frequency alternations), WP-SPIHT introduces smearing effect, which is not so noticeable in SPIHT image. In Fig. 19 we can see that in SPIHT image vertical lines are lost and in WP-SPIHT are still visible. For other textures from Brodatz album similar results are achieved.

Possible application of WP-SPIHT algorithm can be found in object-based wavelet image coding system where different image regions can be coded separately with its own compression ratio. In this approach WP-SPIHT can be employed for coding of texture regions of

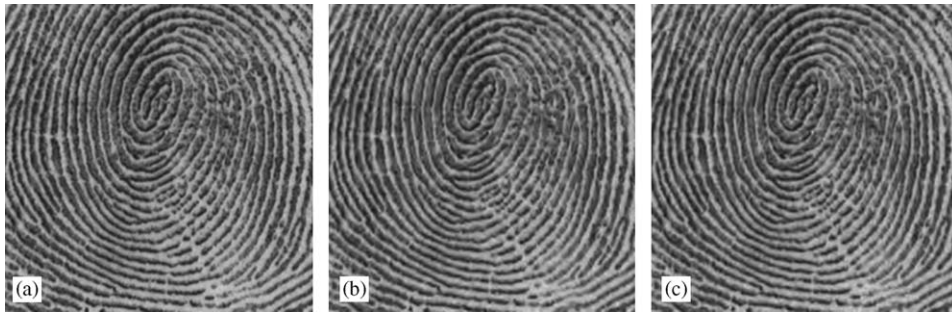


Fig. 17. (a) Original Fingerprints, (b) SPIHT: decoded Fingerprints, 0.25 bpp, (c) WP-SPIHT: decoded Fingerprints, 0.25 bpp.

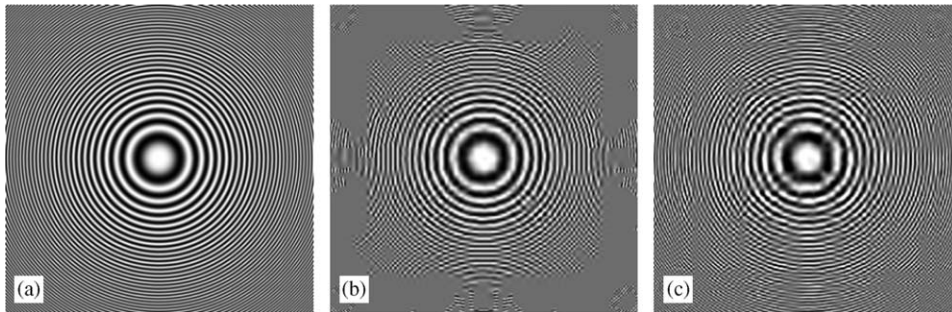


Fig. 18. (a) Original Zone, (b) SPIHT: decoded Zone, 0.25 bpp, (c) WP-SPIHT: decoded Zone, 0.25 bpp.

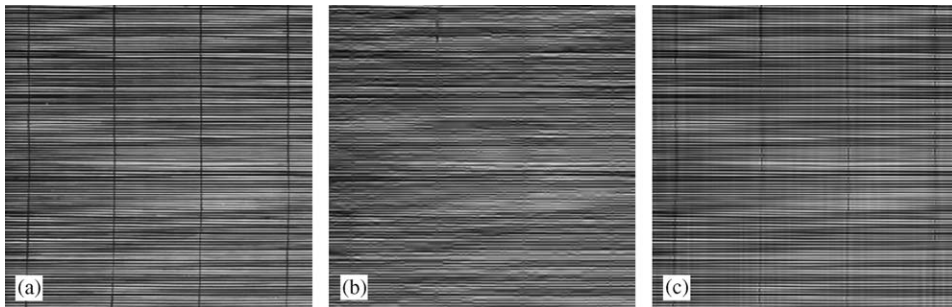


Fig. 19. (a) Original texture D49, (b) SPIHT: decoded D49, 0.25 bpp, (c) WP-SPIHT: decoded D49, 0.25 bpp.

an image and SPIHT for other regions. Moreover, WP-SPIHT algorithm can be used in applications where excellent texture coding performance is essential such as compression of satellite/remote sensing images or medical images for telemedicine, where use of WP-SPIHT algorithm can lead to significant results and improved diagnosis.

5. Conclusion

Efficient set of rules for establishing zerotree structures when used with WP decomposition is presented. The proposed solution enables the modification of popular SPIHT scheme, called WP-SPIHT—a combination of WP as a decomposition method with SPIHT as an image compression scheme. The compression performance of WP-SPIHT has been compared to SPIHT both visually and in terms of PSNR. WP-SPIHT significantly outperforms SPIHT for textures. For natural images, which consist of both smooth and textured areas, the chosen cost function used in WP is not capable of estimating correctly the true cost for a case when the subband is encoded with SPIHT. For those images the PSNR performance of WP-SPIHT is usually slightly worse. As opposed to wavelets, wavelet packet basis might not necessarily produce coefficients that help towards success of the zerotree quantization. Using the entropy as a criterion for the best basis selection can result into many coarse scale high frequency subbands. If a coefficient somewhere at the bottom of the zerotree is found to be significant, the parent nodes need to be encoded even if some of them are insignificant. One way to improve those results would be in designing an advanced cost metric that would take into account the characteristics of SPIHT algorithm and provide optimal distortion value for a given bitrate.

References

- [1] Antonini M, Barland M, Mathieu P, Daubechies I. Image coding using the wavelet transform. *IEEE Transactions on Image Processing* 1992;2:205–20.
- [2] Grgic S, Grgic M, Zovko-Cihlar B. Performance analysis of image compression using wavelets. *IEEE Transactions on Industrial Electronics* 2002;48:682–95.
- [3] Grgic S, Kers K, Grgic M. Image compression using wavelets. *Proceedings of the IEEE international symposium on industrial electronics, ISIE'99, Bled, Slovenia, 12–16 July 1999*. p. 99–104.
- [4] Hilton ML, Jawerth BO, Sengupta A. Compressing still and moving images with wavelets. *Multimedia Systems* 1994;2:218–27.
- [5] Lewis AS, Knowles G. Image compression using the 2-D wavelet transform. *IEEE Transactions on Image Processing* 1992;1:244–50.
- [6] Taubman D, Marcellin MW. *JPEG2000 image compression: fundamentals, standards and practice*. Dordrecht: Kluwer Academic Publishers; 2002.
- [7] Martin K, Lukac R, Plataniotis KN. Binary shape mask representation for zerotree-based visual object coding. *Proceedings of the Canadian conference on electrical and computer engineering, CCECE/CCGEI 2004, Niagara Falls, Ont., Canada, 2–5 May 2004*, p. 2197–200.
- [8] Martin K, Lukac R, Plataniotis KN. Efficient encryption of wavelet-based coded color images. *Pattern Recognition* 2005;38:1111–5.
- [9] Coifman RR, Wickerhauser MV. Entropy based algorithms for best basis selection. *IEEE Transactions on Information Theory* 1992;38:713–8.
- [10] Ramchandran K, Vetterli M. Best wavelet packet bases in a rate distortion sense. *IEEE Transactions on Image Processing* 1993;2:160–75.
- [11] Xiong Z, Ramchandran K, Orchard MT. Wavelet packet image coding using space-frequency quantization. *IEEE Transactions on Image Processing* 1998;7:892–8.
- [12] Meyer FG, Averbuch AZ, Stromberg JO. Fast adaptive wavelet packet image compression. *IEEE Transactions on Image Processing* 2000;9:792–800.
- [13] Said A, Pearlman WA. A new fast and efficient image codec based on set partitioning in hierarchical trees. *IEEE Transactions on Circuits and Systems for Video Technology* 1996;6:243–50.
- [14] Shapiro JM. Embedded image coding using zerotrees of wavelets coefficients. *IEEE Transactions on Signal Processing* 1993;41:3445–62.
- [15] Kim BJ, Xiong Z, Pearlman WA. Low bit-rate scalable video coding with 3-D set partitioning in hierarchical trees (3-D SPIHT). *IEEE Transactions on Circuits and Systems for Video Technology* 2000;10:1374–87.
- [16] Cho S, Pearlman WA. A full-featured, error-resilient, scalable wavelet video codec based on the set partitioning in hierarchical trees (SPIHT) algorithm. *IEEE Transactions on Circuits and Systems for Video Technology* 2002;12:157–71.
- [17] Mukherjee D, Mitra SK. Vector SPIHT for embedded wavelet video and image coding. *IEEE Transactions on Circuits and Systems for Video Technology* 2003;13:231–46.
- [18] Farshchian M, Cho S, Pearlman WA. Optimal error protection for real time image and video transmission. *Proceedings of the 2004 IEEE international conference on acoustics, speech, and signal processing, ICASSP 2004, Montreal, Canada, 17–21 May 2004*, IV-625–IX-28.
- [19] Kim J, Mersereau RM, Altunbasak Y. A multiple-substream unequal error-protection and error-concealment algorithm for SPIHT-coded video bitstreams. *IEEE Transactions on Image Processing* 2004;13:1547–53.
- [20] Kassim AA, Lee WS. Embedded color image coding using SPIHT with partially linked spatial orientation trees. *IEEE Transactions on Circuits and Systems for Video Technology* 2003;13:203–6.
- [21] Bouridane A, Khelifi F, Amira A, Kurugollu F, Boussakta S. A very low bit-rate embedded color image coding with SPIHT. *Proceedings of the 2004 IEEE international conference on acoustics, speech, and signal processing, ICASSP 2004, Montreal, Canada, 17–21 May 2004*, p. III-689–III-92.
- [22] Alatan AA, Zhao M, Akansu AN. Unequal error protection of SPIHT encoded image bit streams. *IEEE Journal on Selected Areas in Communications* 2000;18:814–8.
- [23] Danyali H, Mertins A. Highly scalable image compression based on SPIHT for network applications. *Proceedings of the 2002 IEEE international conference on image processing, ICIP 2002, Rochester, NY, USA, 22–25 September 2002*, p. I-217–I-220.
- [24] Fang JT, Shyu WL, Wu CS. Clustering SPIHT output bits for wireless communications. *Electronics Letters* 2003;39: 235–6.

- [25] Danyali H, Mertins A. Flexible, highly scalable, object-based wavelet image compression algorithm for network applications. *IEE Proceedings—Vision, Image and Signal Processing* 2004;151:498–510.
- [26] Rajpoot NM, Wilson RG, Meyer FG, Coifman RR. Adaptive wavelet packet basis selection for zerotree image coding. *IEEE Transactions on Image Processing* 2003;12:1460–72.
- [27] Ramchandran K, Vetterli M, Herley C. Wavelets, subband coding, and best bases. *Proceedings of the IEEE* 1996; 84:541–99.
- [28] Brodatz P. Textures: a photographic album for artist and designers. New York: Dover Publications; 1966.
- [29] <http://www.sprljan.com/nikola/matlab/ztree.html>